Torsional shear strength behavior of advanced glass-ceramic sealants for SOFC/SOEC applications

M. Ferraris¹, S. De la Pierre¹, A. G. Sabato¹, F. Smeacetto¹, H. Javed², C. Walter², J. Malzbender³

- 1 Politecnico di Torino, Department of Applied Science and Technology DISAT, Institute of Materials Physics and Engineering, 10129 Torino, Italia
- 2 Sunfire GmbH, Gasanstaltstraße 2, 01237 Dresden, Germany
- 3 Forschungszentrum Jülich GmbH, Institute of Energy and Climate Research, IEK-2, 52425 Jülich, Germany

Abstract

Since reliable long term operation of SOFC and SOEC devices depends critically on the mechanical behavior of the sealant material, the current work focuses on the characterization of the shear strength by a torsion test of two different glass-ceramic sealants that are used to join Crofer22APU substrates in an application relevant configuration. The two glass-ceramic sealants differ in terms of characteristic temperatures and crystalline phases with possible impications on the joining behavior. Statistically identical shear stress values were measured at room temperature for joined hourglasses of different size with both sealants, thus confirming a size independence of the measured strength values. Experimental post-test examination results confirm that the interfaces play a strong role regarding the measured shear strength and provide important insights with respect to integration of metallic and glass-ceramic components in SOFC/SOEC stacks.

Keywords: Torsion; SOFC; SOEC; glass-ceramics; sealants; microstructure; mechanical properties;

1. Introduction

The interest in solid oxide fuel/electrolysis cells (SOFCs/SOECs) as electrochemical devices to convert chemical energy of fuels into electricity and vice versa has increased in recent years [1, 2, 3]. Main focus of works has been the planar design due to its higher power output, where typically individual cells are connected together in series to form a stack [4]. Typical temperature ranges are 650 °C to 850 °C [5], where recently long term operation times exceeding 70000 h have been verified [6].

The ceramic cell and metallic interconnects are joined by sealant materials, where, although in some cases metallic materials have been used [7], mostly glasses and in particular glass-ceramic materials are being used [5, 6, 8, 9]. As a consequence of thermal and chemical strains, normal and/or shear stresses arise: this also happens in case of thermal gradients during thermal cycling and even in case of steady state operation [10]. These stresses as well as additional clamping loads [10] can lead to damage and failure, where mobile applications appear to be more critically affected, due to the associated larger number of in-operational thermal cycles [11].

The sealing materials have been identified as a critical component in various studies, since they have to join components and warrant hermetically separation of fuel and oxygen [12]. Therefore, mechanical issues of the sealant material have a serious impact on performance and degradation rate [12]. Although a number of works have been dedicated to evaluate the sealants under tensile- and/or bending-dominant loading condition [13], extensive experimental work has been conducted to evaluate the fracture toughness [8], fracture strength [14] and creep behavior [15], however, only a limited number of studies exist on shear strength evaluation, which appears to be the most application relevant loading condition [16, 17], where especially the application relevant elevated temperature behavior received only minor attention [18].

According to literature, the mechanical properties of the joints, such as strength significantly depends on the testing method. Selçuk et al. [19] investigates the shear strength of glass—ceramic sealants by single lap offset (SLO) under compression, single lap (SL) under compression and asymmetrical 4-point bending test (A4PB). Three different testing methods results in a significant variation in the apparent shear strength, in particular, in the SLO configuration relatively lower strength was obtained due to higher normal tensile stresses perpendicular to the joint.

The mechanical stability of the glass-ceramic based joints can be critical at high temperatures, especially during cooling cycle once the temperature is lower than Tg. Different researchers have analyzed mechanical properties of glass-ceramics at room and high temperatures. For instance, Stephens et al. [20] tested a barium–calcium–aluminosilicate-based glass-sealing material (G18) under tensile and torsion conditions, to analyze the interfacial shear strength between the G18 glass and the Crofer22APU. A noticeable reduction (50%) in the mechanical strength of joint was observed with an increase in temperature from 25 °C to 800 °C.

The torsion test on hourglass-shaped specimens appears to be a convenient and promising method to assess the shear strength with only a minor effect of unwanted addition stress components [16, 17, 21, 22], hence, in the current work shear stresses are measured by torsion test for two different sealants by measuring their behavior at room temperature and at application relevant temperatures. The results are supported by extensive post-operation characterizations by using electron microscopy and compositional analysis on the fracture surfaces.

2. Experimental

The two sealants (abbreviated as GC1 and GC2) have been prepared by melt-quenching process at 1500 °C, 1 hour; starting products (oxides and carbonates) have been carefully mixed and then melted in air furnaces in platinum-rhodium crucibles. The compositions for both sealants are reported in Table I; the properties of GC1 have been published elsewhere [23] and also summarized in Table I. Both sealants have been obtained by casting on a brass plate and the transparent glasses ground to less than 38 microns for the following characterizations. The glass transistion temperature (T_g) was measured at a heating rate of 5 °C/min on the powdered as-cast glasses by differential thermal analysis (DTA) (Netzsch, EOS, Selb, Germany). The softening temperature (T_s) and coefficient of thermal expansion (CTE) were measured by hot-stage microscopy (HSM) (Expert System solutions, Modena, Italy) and dilatometry, respectively, on bulk cylindric glass-ceramic samples of 5 mm height obtained by sintering GC1 and GC2 powders with the same thermal treatment used for their joining processes. The crystalline phases in both glass-ceramics were analyzed by X-ray diffraction XRD (Bruker AXS D8 Advance, Karlsruhe, Germany). Both sealants have been powdered and sieved to particle size < 38 microns and mixed with a minimum amount of ethanol to obtain a slurry suitable to be applied by a spatula on the surfaces of the two metallic parts to be joined.

The hour-glass shape and size of the joined samples are shown Figure 1: two kind of hour-glass shaped samples, both made of the same steel (Crofer 22 APU, ThyssenKrupp VDM GmbH, Germany), have been machined in the hour-glass shape, cut in two parts, then joined by applying the sealant slurry between the two parts: TGH-5 samples, Figure 1 (a), have a joined region diameter of 5 mm, a total height of 3 mm whereas THG-25 samples, Figure 1 (b) have been designed by multiplying the previous diameter and curvature radius by five: the joined region diameter is hence 25 mm and the total height is 11 mm as fixed by the thickness of available material. A tolerance range of \pm 0.1 mm is to be considered.

Prior to the joining process with GC1, the half hour-glasses have been pre-oxidized at 950 °C for two hours in a chamber furnace in air to aid bonding onto the oxide scale. Afterwards, they have been then joined by GC1 slurry in a tubular furnace (Carbolite Gero STF 16/180 for THG-5 and GHA 12/300 for THG-25), in Ar atmosphere at temperature of 850°C, joining time 30 min, with the help of a graphite sample holder, to keep the samples in place.

Since pre-oxidation was not necessary for GC2 sealant, the slurry was used to join as received Crofer22APU half hour-glasses by heat treatment at 950°C, in a muffle furnace, joining time one hour, in air atmosphere: in this case, an alumina sample holder was used to keep samples in place.

Both joining processes have been done without applying any pressure, which appeared not to be necessary for these sealant materials. The thickness of each joint has been characterized based on the thickness difference before and after joining the two half hour-glasses and ranged between 120 and 220 microns; joined hour-glasses have been tested in torsion at room temperature at Politecnico di Torino, Italy (POLITO) (TGH-5 only) and at Forschungszentrum Jülich, Germany (FZJ) (both THG-5 and THG-25); tests at operation relevant elevated temperature (700-800°C) have been done only at Forschungszentrum Jülich (both THG-5 and THG-25) (Figure 2).

The torsion tests at POLITO were performed in a universal testing machine (Zwick 100, Zwick/Roell, Hertfordshire, UK), where the load was applied until fracture occurred. The torsion load was applied using a rotating disc fixture with a wire equipped in the mechanical test frame. The crosshead speed was 0.5 mm min ⁻¹ with an estimated rotation speed of 0.010 rad min⁻¹ [16].

In the torsion tests at FZJ the specimens were twisted with a speed of ~ 4° min⁻¹ until fracture occurred [18].

A round-robin test with the two torsion machines has been done using epoxy adhesive bonded steel hourglasses (THG-5) prior to this work, to test the comparability of the obtained results.

The joined samples fracture surfaces and interfaces have been observed by FESEM (Merlin, ZEISS) and their composition measured by EDS.

3. Results and discussion

Both glass compositions were formulated so that the resulting glass-ceramics have crystalline phases with suitable CTE ($10-14 \times 10^{-6} \text{ K}^{-1}$). Besides that, the glass compositions were further tuned using the SciGlass® database (Science Serve GmbH, Sciglass 6.6 software, Newton, MA, USA) in order to obtain glass transition temperatures between 600-700°C as main criteria for the sealants

GC1 is a silica based glass containing Na, Mg and K oxides to adjust glass viscosity, decrease characteristic temperatures and increase the wettability on the metallic interconnect. This particular composition was also chosen for its good sintering behaviour at a joining temperature, as reported in [23].

Concerning CTE evolution as a function of time, the properties of GC1 have been published in [20]. XRD analysis of the glass-ceramic and Rietveld refinement showed diposide as the main crystalline phase and substantial amount of a residual amorphous phase (58%wt) after the joining process. Interfacial compatibility with Crofer22APU and YSZ was found to be very good, also after 500 h of thermal cycling (RT-800) in air (no cracks formation, interactions, or failure were observed) thus consequently demonstrating an excellent stability of the GC1 system in terms of thermomechanical properties.

The GC2 is a silica based glass with BaO as main modifier and without alkali metal oxides. BaO is most commonly used modifier, as it improves the wettability and CTE of glass [24]. Moreover, in the silica based glasses, BaO tends to form $BaSi_2O_5$ phase, having CTE in the range of 11-14 x 10^{-6} K⁻¹, necessary to obtain a glass-ceramic with suitable CTE for SOFC applications. However, BaO based glass systems are usually affected by the formation of high CTE BaCrO₄ phase [25,26]. The formation of BaCrO₄ took place due to chemical reaction between Ba from glass and Cr from steel. The presence of high CTE BaCrO₄ phase mostly results in the crack formation or delamination at steel/glass-ceramic interface, thus adversely affecting the mechanical stability of the joining area. In this context, in GC2, the SiO_2/SiO_2 +BaO ratio has been adjusted to 0.68 to ensure the formation of high CTE BaSi₂O₅ phase and to avoid/minimize the formation of high CTE BaCrO₄ and cristobalite phase (SiO₂) with different polymorphs. In addition to BaO, 7 mol% of CaO has been also added to maintain the CTE and viscosity of the residual glassy phase. The Al₂O₃ concentration was kept at 4 mol% to avoid the formation of low CTE celsian phase [27].

This particular hour-glass geometry, Figure 1 (a), labelled as THG-5, has been modelled and experimentally verified in several laboratories as one of the very few suitable methods being able to provide shear strength under torsional loading for a wide range of joined samples [23].

Results obtained by this test must be carefully analysed with the aid of advanced finite element simulation before using the derived values as shear strength values. However, in this current particularly favorable case, i.e. when the joining material is purely brittle and the fracture due to torsion load originates and propagates in the joined region only, the maximum of the torsion curves can be used to calculate the shear strength of the joint, according to the analytical formula for the shear strength of the joint, as in eq. 1 and 2 [16]:

$$\tau_{max} = Shear \, Strenght = \frac{M_{max}}{J \cdot R_e}$$
Eq. 1

with:

$$J = \frac{\pi R_e^4}{2}$$
 Eq. 2

where τ_{max} is the shear strength, M_{max} the maximum torque, J the polar moment of inertia and R_{e} the outer radius of the joined area.

The area of the hourglass TGH-5 geometry was multiplied by five in order to obtain larger samples (referred to as THG-25) for easier handling and in order to check if there is any size effect as typically observed in the fracture strength of brittle ceramic materials; it has to be emphasised that the THG-5 hourglass was designed a decade ago within an activity that focused on joining materials for nuclear applications and miniaturized samples were needed to test several samples in the same nuclear irradiation capsule of limited size [28, 29]. In fact, joining such small samples as here in the case of THG-5 can be an issue, in particularly when they are joined one by one: hence, this study aimed towards checking if larger samples of the same geometry (THG-25) still give the same shear strength of smaller ones (THG-5). If this is the case, the measured value is size independent and can be correctly defined and used as shear strength.

Figure 2 illustrates the torsion test equipment available at FZJ [30, 31], which is suitable for RT and HT tests; a larger magnification of a THG-25 joined sample inside the fixture is visible in Figure 2 (b); a similar equipment is operative at POLITO for room temperature test only [28].

It has been verified that the two torsion machines give statistically identical results on the basis of tests performed on more than twenty epoxy adhesive bonded steel hour-glasses (THG-5) within an internal round-robin test between the two laboratories, that was performed prior to this work as preliminary activity; since it is out of the scope of the current work, it is not reported here. Similar statistically identical results were obtained with the POLITO torsion machine within a previous round-robin test done with two similar torsion equipment, one being at Kyoto University (Japan) and another one at ORNL (USA) [28].

In order to fully understand the torsion test results both at room and high temperature, it is important to consider potential reactions and transformations which might occur during the joining processes. Since the joining process with GC1 slurry has been done in Ar atmosphere to avoid unwanted oxidation of the graphite sample holder, a pre-oxidation process of steel counterparts was necessary prior to the joining, also with the aim to increase adhesion and compatibility between steel and GC1 sealant. Associated with this oxidation an oxide scale with a thickness of about one micron was verified to form on the steel during this pre-oxidation process, at 950 °C for two hours in air [22, 23].

Contrary to this, the joining process with the GC2 slurry could be done in a muffle furnace in air, and the oxidation process of steel took place hence directly during the joining procedure, at 950 °C for one hour.

Moreover, both sealants partially crystallized to glass-ceramics (GC1 and GC2) during the joining process, their main crystalline phases and characteristics temperatures are presented in Table I. The GC1 has diopside (CaMgSi₂O₆) while GC2 has sanbornite (BaSi₂O₅) as main crystalline phases. As shown in table I, the as-joined GC1 and GC2 has CTEs of 10.9 and 11.4 x 10^{-6} K⁻¹ respectively, thus closely matching with that of Crofer22APU and suitable for SOFC/SOEC application. For both glass-ceramics, the oxide scale with a thickness >1 μ m has been observed at Crofer22APU surface as investigated by SEM, Figure 3(a), and is composed mainly of Cr₂O₃, as investigated in previous studies carried out on same steel under similar joining treatments [27].

Figure 3 summarizes the post-test observations for GC1 joined THG-5 after torsion tests at room temperature: Figure 3(a) is a cross-section and Figure 3 (b) presents the visual appearance of a typical fracture surface after torsion for a GC1 joint specimen. Figure 3 (c) sketches the typical fracture propagation for these samples, showing the *adhesive* failure behavior of these joints, i.e. with GC1 on *one fracture surface only*, as it can be observed in Figure 3 (d) by complementary SEM-EDS information. The measured average shear strength for these THG-5 joints corresponded to 35 ± 9 MPa.

The same behavior and failure morphology was also observed for the larger THG-25 tested in torsion at room temperature and the associated measured average shear strength was in this case 28 ± 6 MPa (pictures showing THG-25 specimens after testing are not reported for brevity, since they are identical to what is reported in Figure 3).

It has to be emphasised that GC1 joined TGH-5 specimens have already been the focus of a previous work and results for specimens tested at RT were reported and discussed in [22]; however, in that test series they yielded a much higher average shear strength (71 \pm 10 MPa). In order to understand this unexpected difference, a comparison of fracture surfaces for the current GC1 joined samples and the previous ones was carefully performed in order to get insight into the reasons of the lower mechanical strength obtained here.

In fact, completely different fracture surfaces were observed and reported in [22]: all THG-5 joined by GC1 and tested at room temperature revealed mixed (adhesive/cohesive) mode fracture surfaces, i.e. with the glass-ceramic present on both sides. On the contrary, all the GC1 joined THG-5 that were tested in the current work showed a purely adhesive behavior as presented in Figure 3, with the fracture propagating between steel and oxide scale.

Despite careful SEM-EDS characterizations of cross-sections and fracture surfaces of several joined samples from both batches (i.e. CG1 joined samples from [22] and from this work), no evidence of different reactions at the interface between GC1 and steel was found. One may suppose that the different adhesion at the interface between steel and GC1 in [22] and in this work is most likely due to different furnaces used to prepare these samples or gas purity used to obtain the previous GC1 joints, resulting in different measured shear strengths.

To confirm this assumption, i.e. that the interface plays a strong role in the shear strength measured by torsion, it is worth noting an interesting behavior regarding torsion tests at room temperature and 600 °C for GC1 joined THG-5, (Figure 4): as expected for a brittle glass-ceramic joining material the typical torque (T, Nm) versus time at room temperature is linear. In this case, the maximum of the four curves was used to calculate the average shear strength of these joints, according to eq.1 and 2, yielding 35 ± 9 MPa.

However, completely different torsion tests curves can be observed in Figure 4 at 600 °C (two curves) for GC1 joined THG-5, with an apparent increase in "torsional strength", which can be explained as follows: when the GC1 joined THG-5 samples were tested at 600 °C, the typical fracture surfaces, (Figure 5) has no clear adhesive failure anymore, but rather a *mixed failure mode*, i.e. with GC1 being present on *both* fracture surfaces. A certain interface strengthening might have occurred, as illustrated in Figure 5 (a), which shows the fracture surfaces after torsion testing of a GC1 joined THG-5 at 600 °C; the apparent *mixed* (i.e. adhesive/cohesive) fracture propagation is sketched in Figure 5 (b), with GC1 being present on *both* fracture surfaces, as verified by SEM-EDS, Figure 5 (c), which also gives evidence of some oxidation (purple zones) on the steel side.

Moreover, due to the viscoelastic behavior of GC1, which is tested in this case at a temperature close to its parent glass transition temperature, but still below its glass ceramic softening temperature (Table I), the curves of the GC1 joined THG-5 tested in torsion at 600 °C (Figure 4) are not linear anymore and their maximum cannot be used to calculate a shear strength of the joints according to eq.1 and 2; however, it can be clearly seen that the "torsional resistance" for these samples increased when shifting from a purely adhesive-and-brittle to a mixed-and-partially viscoelastic failure mode.

In some cases linear/brittle or non-linear/ductile behavior have been reported and discussed for epoxy adhesives tested in torsion with this kind of hour-glass geometry [32]: also for epoxy adhesives, when the torsion curves are not perfectly linear, their maximum cannot be used to calculate the shear strength of the joints according to eq.1 and 2; however, also for epoxy adhesives it can be clearly seen that the "torsional resistance" increases when the adhesive has a mixed and partially viscoelastic failure mode.

An increase in "torsional resistance" has been also reported for adhesively joined samples, when their interface strength was increased by pre-etching of substrate [33].

Table II summarizes all torsion results obtained with GC1 at room temperature along with information regarding the fracture mode: when GC1 is strongly bonded to steel it shows a mixed adhesive/cohesive fracture mode and gives a shear strength of 71±5 MPa at room temperature.

When the adhesion of GC1 is not optimal and its interface with steel is weak, then the fracture mode is adhesive (Figure 3) and the shear strength at room temperature (between 28 and 35 MPa) is a measure of the interface shear strength, which is about a half of what measured for the same GC1 sealant bonded by a stronger interface (71 ± 5 MPa), which fails in a mixed failure mode. It is worth emphasing that the shear strength for this (weak) interface is size independent, i.e. approximately the same values ranging between 28 and 35 MPa were obtained with both THG-5 and THG-25 geometries at room temperature.

Torsion tests on CG1 joined samples at 600°C evidenced two important features respect to samples tested at room temperature: an interface strengthening might have occurred during heating the samples at 600°C, thus the fracture mode changed *from adhesive* (Figure 3) *to mixed* (Figure 5); moreover, curves in Figure 4 changed from elastic to elasto-plastic, due to the viscoelastic behavior of the glass-ceramic sealant at 600°C. Both features concurred in increasing the "torsional resistance" of the joined samples.

In order to verify what has been discussed above, the results obtained with the second glass-ceramic sealant (GC2) are of some interest: GC2 was used to join hour-glass specimens made of the same steel, with the same geometry (THG-5 and THG-25), but it has higher characteristic temperatures than GC1 (Table I). With GC2 the preoxidation treatment was not carried out; an alumina sample holder was used for the joining process in air.

Figure 6 (a,b) shows the polished cross-sections of as-joined GC2 confirming a homogenous microstructure and strong adhesion with Crofer22APU. Figure 6 (c) represents the fracture surfaces after torsional testing obtained for both THG-5 and THG-25 GC2 joined samples at room temperature, which yielded τ = 49 ± 10 MPa and τ = 45 ± 17 MPa, respectively; Figure 6(d) sketches the *mixed* fracture propagation behavior, with GC2 partially present on *both* fracture surface, as verified via SEM-EDS, in Figure 6 (e) (pictures refer to THG-25).

It is evident in this case that the interface was strong enough to avoid a complete adhesive behavior: on the contrary, a *mixed* fracture mode was always found: consequently, the shear strength for GC2 joined hourglasses correspond to values ranging between 45-49 MPa for both THG-5 and THG-25 (Table II). Similar post mortem results have been reported by Javed et al [34]. where mixed fracture was observed when Crofer22APU/glass-ceramic/Crofer22APU joints were investigated under shear load, and was attributed to strong adhesion of glass-ceramic with Crofer22APU substrate.

It is worth noting in this context that statistically identical shear strength values were obtained for GC2 joined hourglasses of both sizes (THG-5 and THG-25), thus confirming the size independence of the measured value, which can hence be defined as *shear strength of GC2 joined Crofer22APU at room temperature*.

Figure 7 is an additional confirmation of the interesting peculiarity of the torsion test discussed in this work: this torsion test seems to be useful in detecting if there is something wrong in the interface strength in a joint: Figure 7(a) shows *anomalous* fracture surfaces that occurred after torsion tests of some GC2 joined THG-5 specimens tested at room temperature, with the fracture propagation mode sketched in Figure 7(b). The GC2 material after the test was *mostly located on one fracture surface* only, as also verified by SEM-EDS in Figure 7 (c) with each region identified. Sample fractured in this mode had an average shear strength lower than *30 MPa* and have been discarded in further analysis, due to possible issues during GC2 joined samples preparation.

Both THG-5 and THG-25 joined by GC2 were also tested in torsion at a temperature higher than expected for these sealants, given their characteristic temperatures: their typical fracture surfaces are shown after testing temperatures of 700 °C, Figure 8 (a) and 800 °C, Figure 8 (b). (pictures refer to THG-25). Their fracture mode can be defined as mixed mode for both temperatures, with the GC2 sealant material being present on both surfaces. In fact, GC2 possesses still a remarkable "torsional resistance" at 700°C, which is lower than its softening point (810°C) (Table I); however, the steel is plastically deformed at 700°C, due to entering the plastic field under torsion, Figure 8 (a).

On the contrary, at 800 °C (Figure 8 b) GC2 was close to its softening point (Table I), therefore its negligible mechanical strength as joining material caused failure of the THG-25 joined samples without plastic deformation of the steel (Figure 8 b). (The same behavior was observed for GC2 joined THG-5 specimens tested at the same temperatures, which is not reported here for brevity).

A typical torque (T, N/mm) versus time curve of a THG-25 joined sample tested at 800 °C is shown in Figure 8 ©, from which the elasto-plastic behavior is evident. Also in this case, the maximum of the curve cannot be used to calculate the shear strength of the joint, but only to give an idea about a "torsional resistance", as discussed above.

Table II summarizes the results obtained with both glass-ceramics as joining materials: accordingly to what has been discussed above, it can be safely stated that the shear strength of these glass ceramic joined steel hour-glasses at room temperature ranges between 50 and 70 MPa, and it is size independent.

Both glass-ceramics retain a remarkable "torsional resistance" up to 700 °C, however, due to the non-linear behavior of these curves, a shear strength cannot be calculated by using the maximum of these curves.

4. Conclusion

This work focused on the shear strength measured by torsion test on two different glass-ceramic sealants are used to join Crofer22APU substrates for SOFC/SOEC stacks.

Statistically identical shear stress values were measured by torsion at room temperature for joined hourglass shaped samples of different size, thus confirming the size independence of the measured shear strength values. Experimental post-test examinations confirmed that interfaces play a strong role regarding the measured shear strength and provide important insights with respect to integration of metallic and glass-ceramic components in SOFC/SOEC stacks.

Acknowledgements

The torsion experiments at Jülich were supported by Ms. T. Osipova and Mr. M. Turiaux. Part of this activity has been done within J-TECH@POLITO (http://www.j-tech.polito.it/).

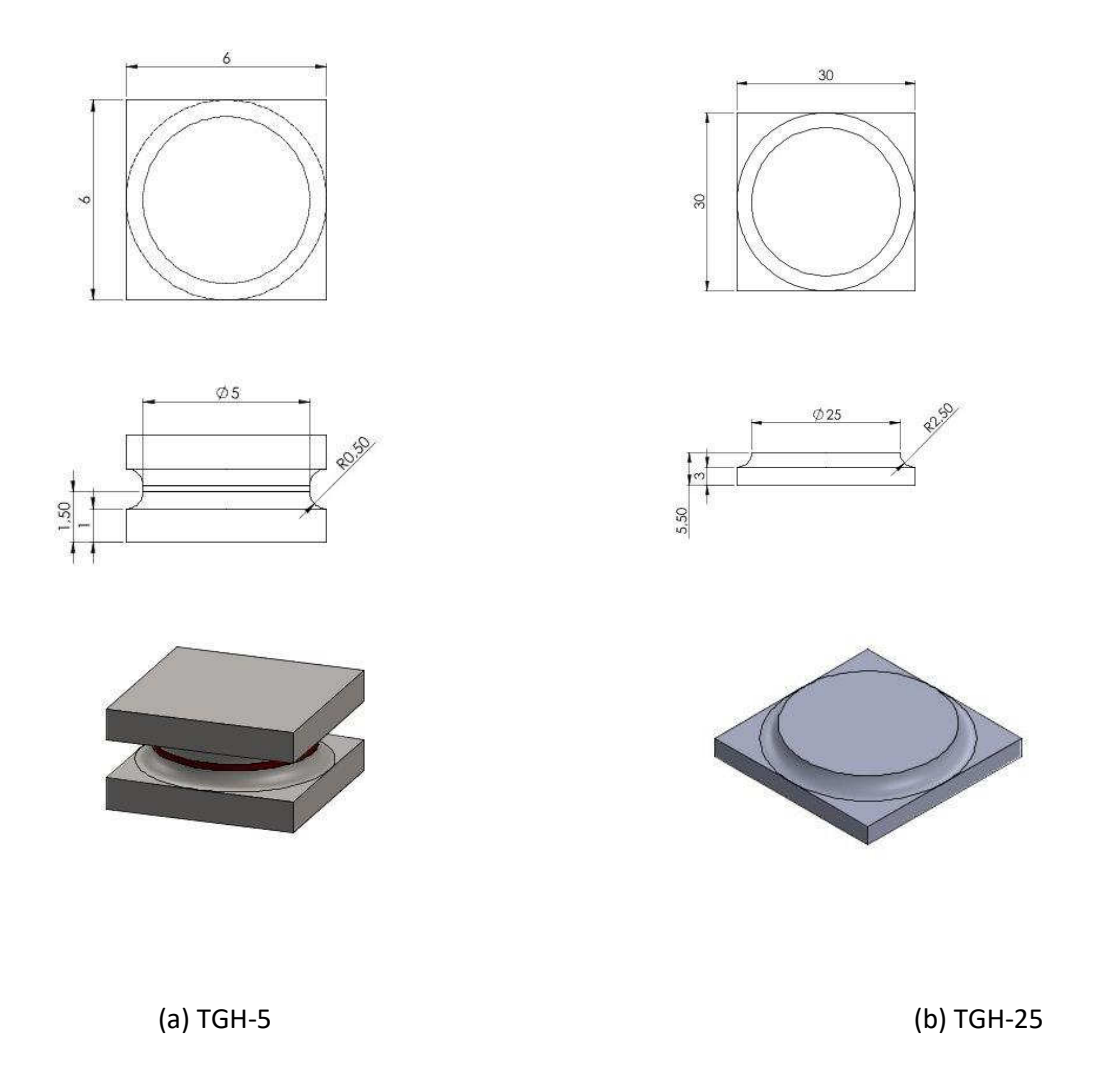


Figure 1: Size of hourglass shaped samples; both of them are made of steel (Crofer 22 APU), machined in the hourglass shape, cut in two parts, then joined by applying the sealant slurry between the two parts: TGH-5 samples (a) have a joined area diameter of 5 mm, a total height of 3 mm; THG-25 samples (b) have been designed by multiplying the previous diameter and curvature radius by five. (half hourglass is shown in figure 1b)

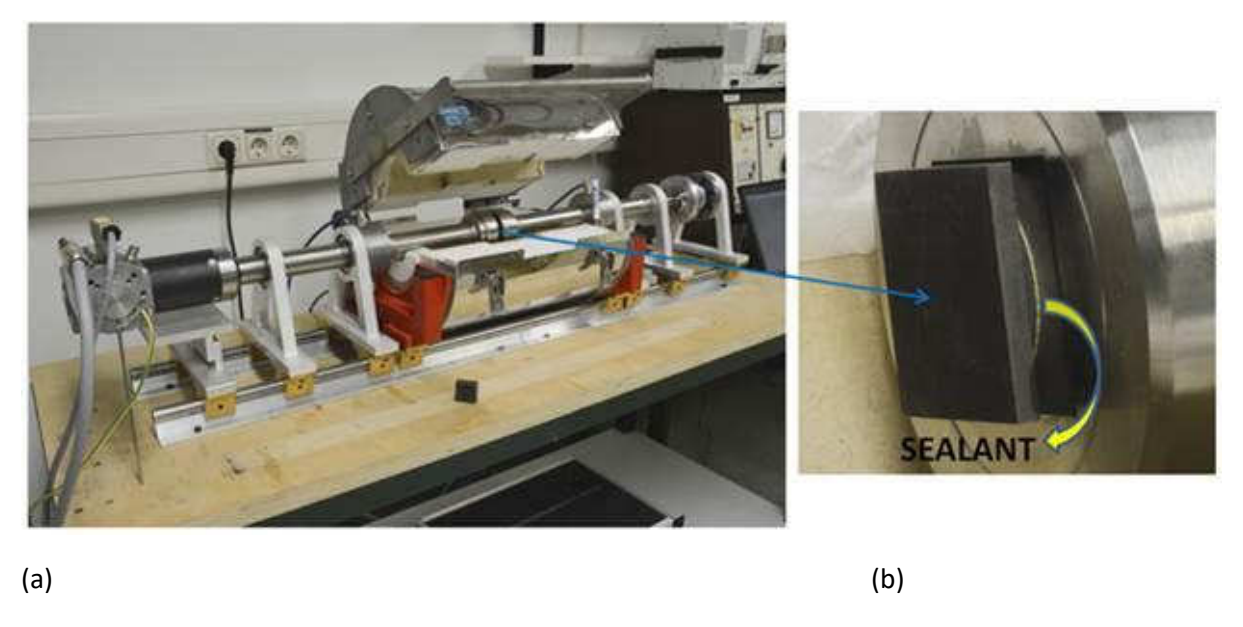
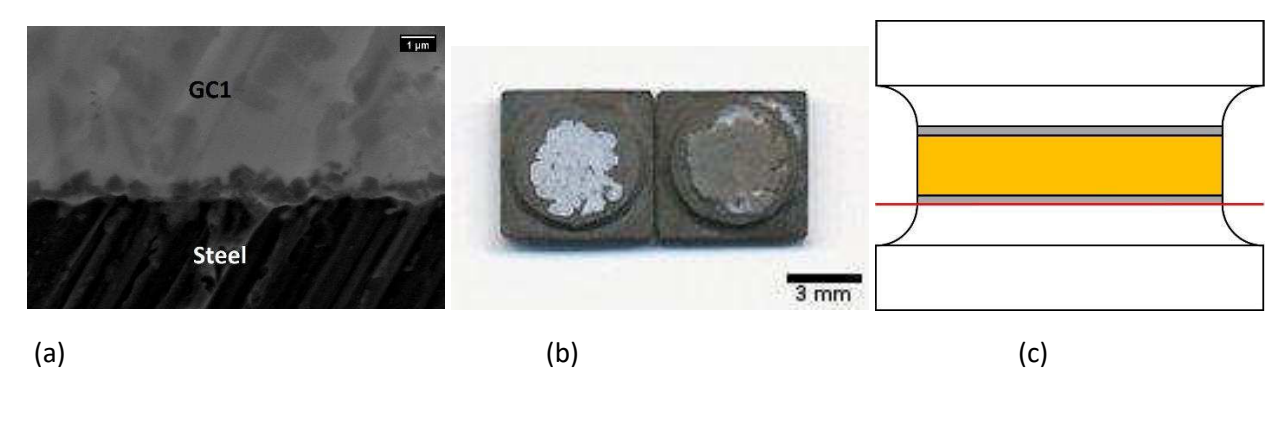


Figure 2: Torsion test equipment at FZJ, suitable for RT and HT tests; particular of the hourglass shaped joined sample inside the fixture (b); a similar equipment is operative at Politecnico di Torino, Italy, for room temperature test only (22).



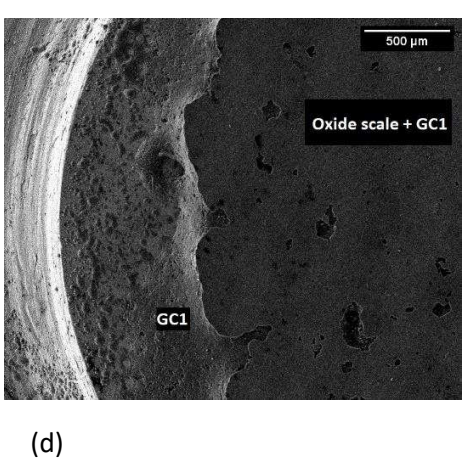


Figure 3: THG-5 joined sample tested at room temperature by glass-ceramic 1 (GC1): (a) polished cross-section; (b) typical fracture surfaces after torsion; (c) fracture propagation sketch (orange=glass-ceramic; grey=oxide scale; red=fracture propagation) showing the *adhesive* behavior, with glass-ceramic 1 (GC1) present on *one fracture surface only*, as observed in (d) by SEM-EDS, with each region identified.

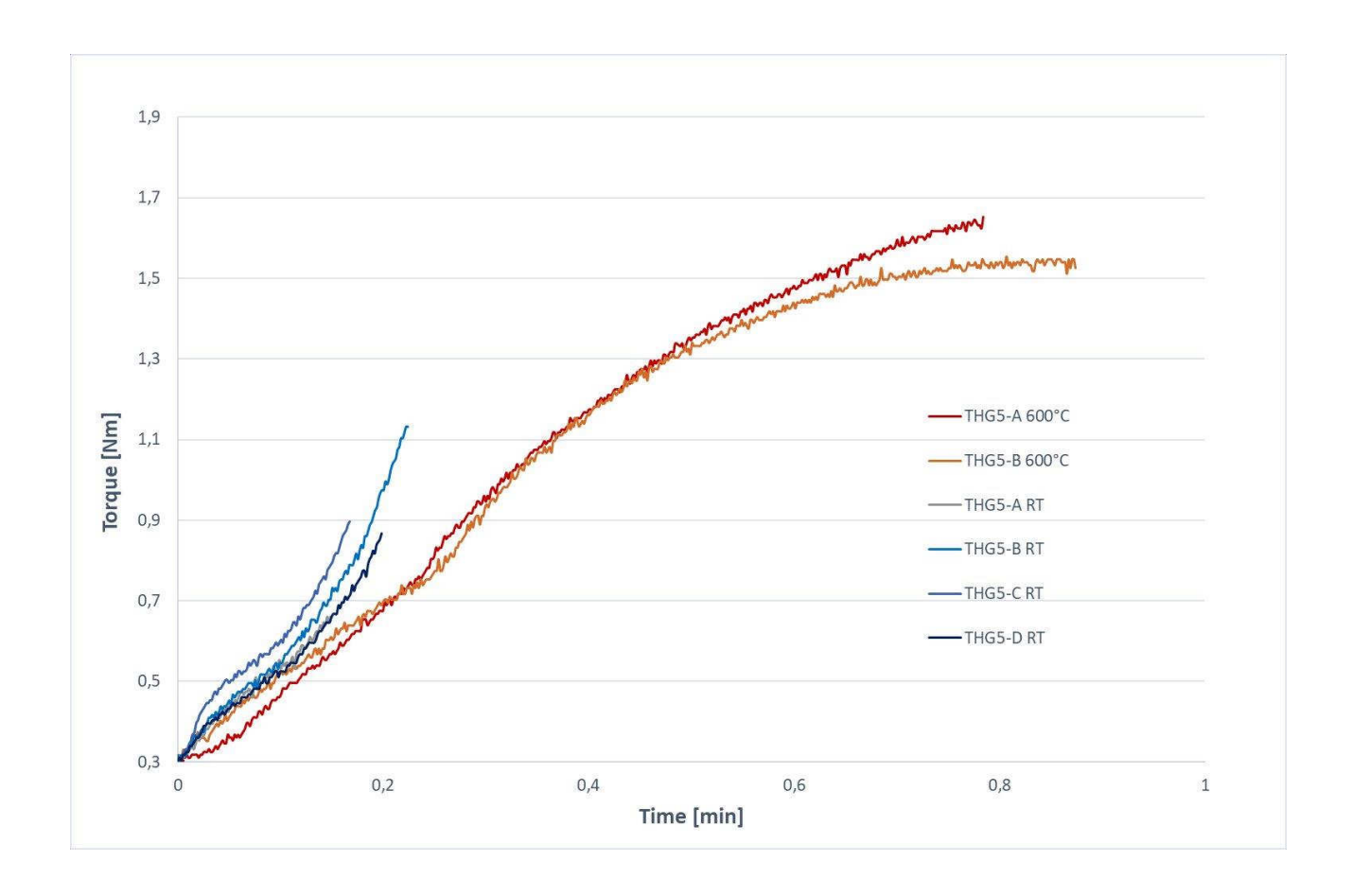
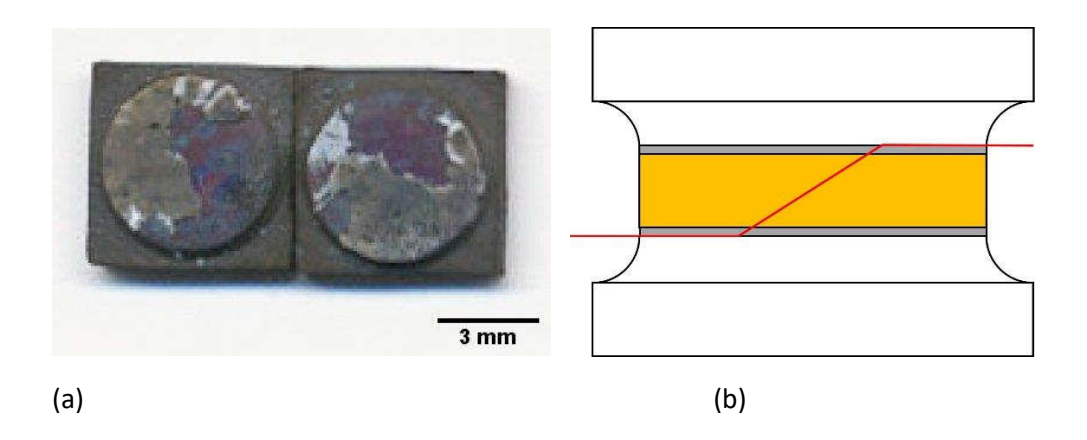


Figure 4: Typical torque (T, N/m) *versus* time (minutes, 4°/min) of THG-5 samples joined by GC1, showing the brittle behavior of the glass-ceramic joining material at room temperature (curves A-D, RT), with the typical fracture surfaces after torsion, (inset). Curves A-B 600°C refer to THG-5 joined samples tested at 600 °C: the elasto-plastic behavior is evident, with the typical fracture surfaces after torsion, (inset).



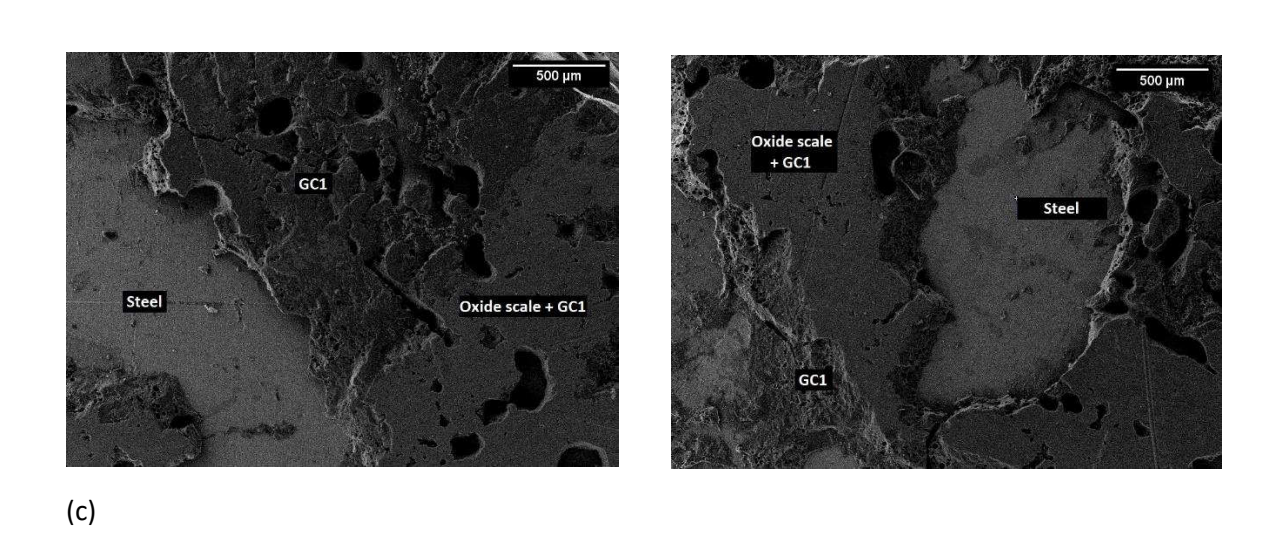


Figure 5: (a) fracture surfaces after torsion for a THG-5 sample joined by GC 1 and tested at 600 °C, showing *mixed* (i.e. adhesive/cohesive) behavior as sketched in (b), with GC1 being present on *both* fracture surfaces, as observed by SEM-EDS (c), with each region identified.

.

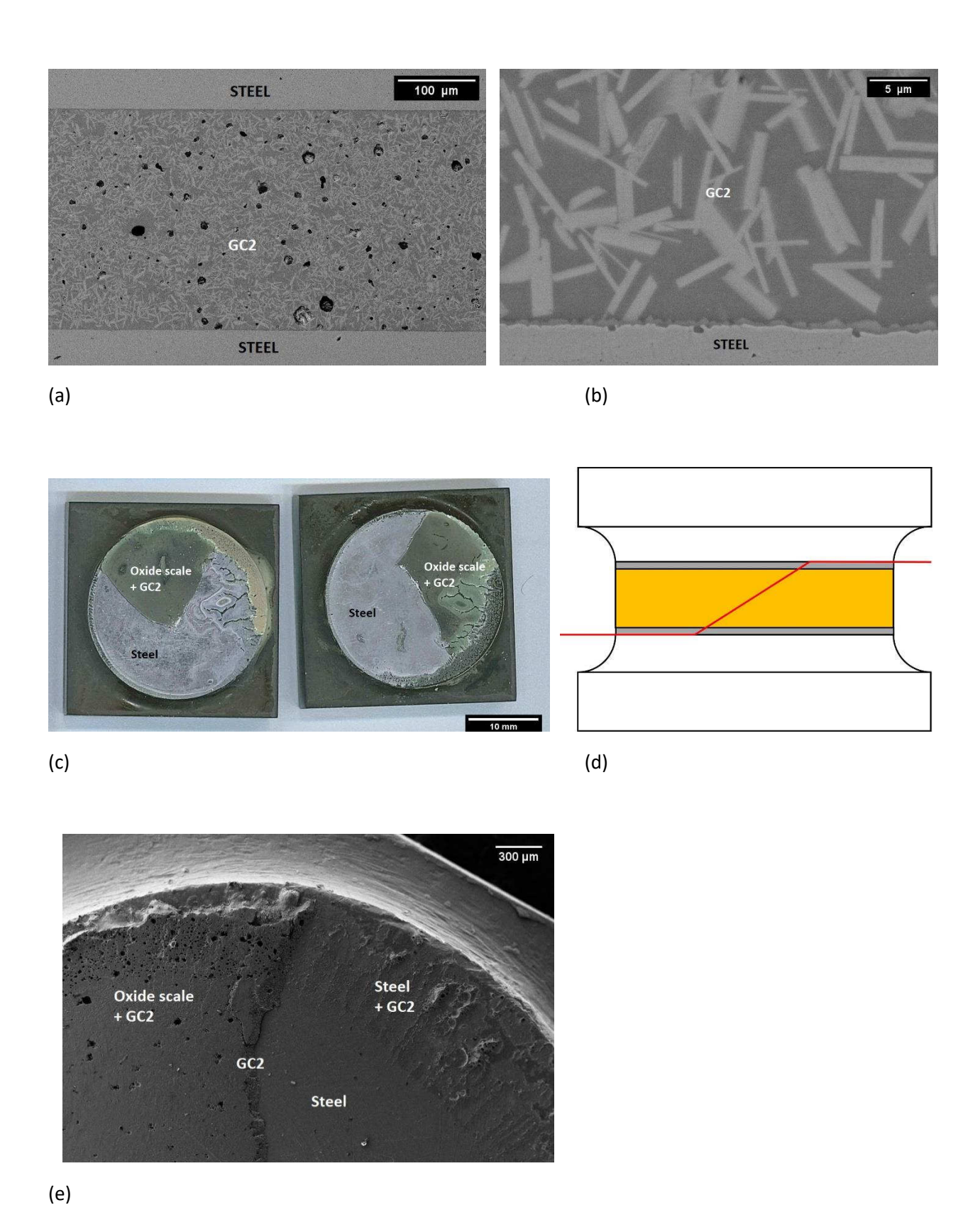


Figure 6: (a,b) typical polished cross-sections and (c) typical fracture surface after torsion for both THG-5 and THG-25 glass-ceramic 2 (GC2) joined samples after test at room temperature (τ = 49 ± 10 MPa and τ = 51 ± 17 MPa, respectively) (pictures refer to THG-25); (d) fracture propagation sketch (orange=glass-ceramic; grey=oxide scale; red=fracture propagation): *mixed* behavior, with GC2 partially present on *both* fracture surface, as verified in (e) by SEM-EDS, with each region identified.

.

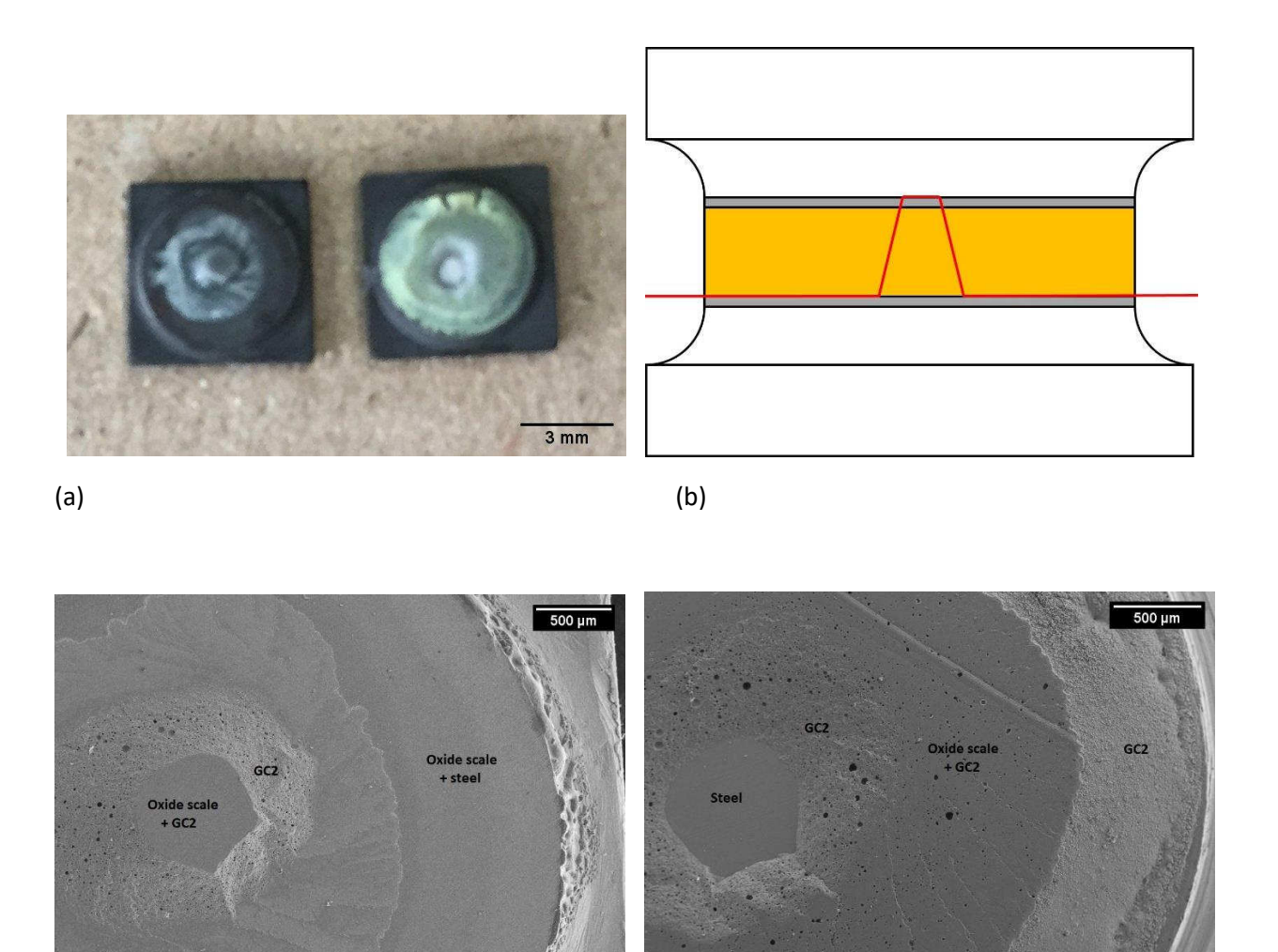
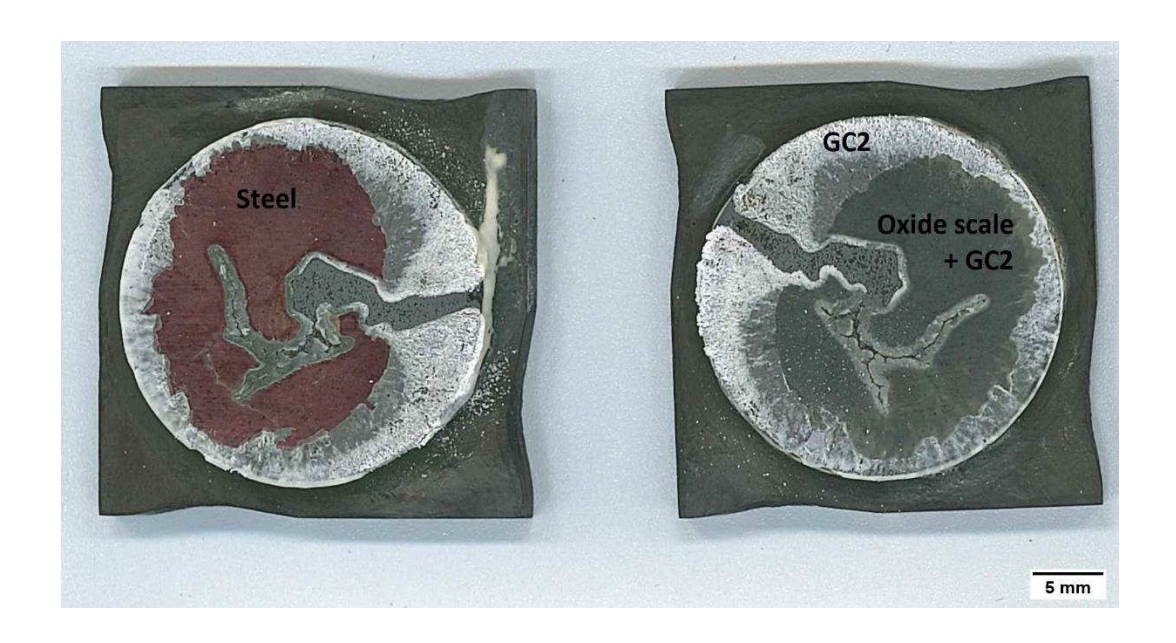


Figure 7: (a) *anomalous* fracture surfaces after torsion for some THG-5 GC2 joined sample tested at room temperature: (b) fracture propagation sketch (orange=glass-ceramic; grey=oxide scale; red=fracture propagation) with GC2 present *mostly on one fracture surface*, as observed by SEM-EDS in (c) with each region identified.

(c)





(b)

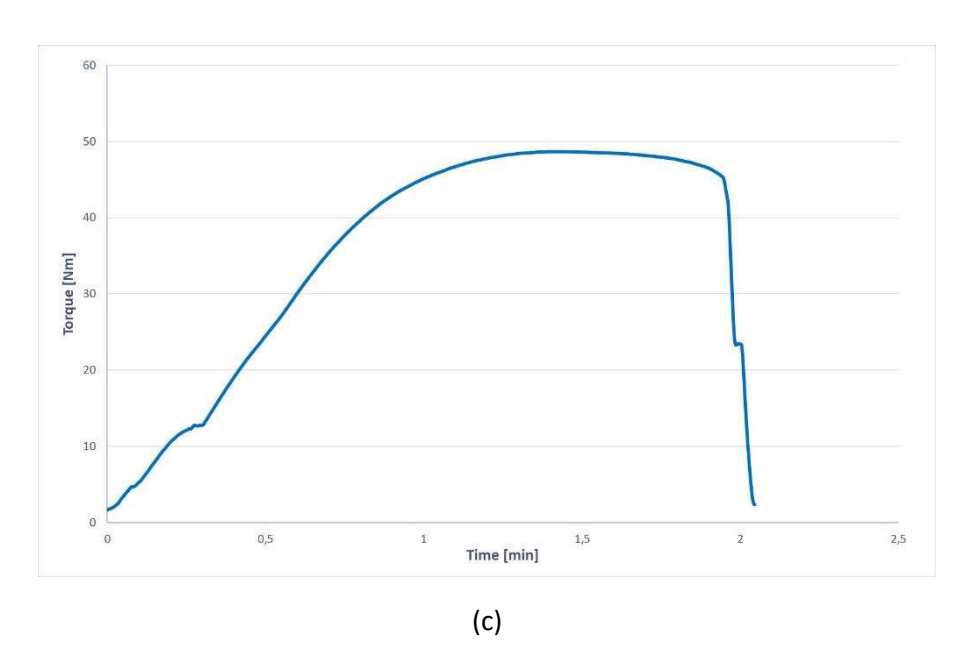


Figure 8: Typical fracture surfaces of both THG-5 and THG-25 joined by GC2 and tested in torsion (FZJ) at 700 $^{\circ}$ C (a) and 800 $^{\circ}$ C (b) (pictures refer to THG-25). Typical torque (T, Nmm) *versus* time (minutes, 4°/min) of a THG-25 joined sample tested at 800 $^{\circ}$ C (c).

		Glass							Glass ceramic					
Mola r %	SiO ₂	B ₂ O ₃	Al ₂ O ₃	CaO	BaO	Na₂O	MgO	K₂O	Y ₂ O ₃	Tg (°C)	Ts (°C)	CTE 10 ⁻⁶ °C ⁻¹ (200-500 °C)	Main crystalline phases	Joining process
GC1 (ref 20)	55.2	0.8	6.7	9.8	0	13.5	12.7	1.1	0.2	605	625	10.9	diopside (CaMgSi ₂ O ₆) ,	Steel oxidation 950°C, 120 min, air 830 °C, 30
														min, Ar
GC2 (ref 21)	55	8	4	7	26	0	0	0	0	677	810	11.4	sanbornite (BaSi ₂ O ₅)	950°C, 60 min, air

Table I Glass and glass-ceramic sealants GC1 and GC2 composition, characteristic temperatures, coefficient of thermal expansion, crystalline phases and joining process conditions. (20, 21)

		Test Temperature (°C)	N° of samples	Type of fracture	Shear strength (MPa)
GC1	THG-5	RT	11	mixed	71 ± 5 (ref 19)
	THG-5	RT	9	adhesive	35 ± 9
	THG-25	RT	5	adhesive	28 ± 6
GC2	THG-5	RT	11	mixed	49 ± 10
	THG-25	RT	3	mixed	45 ± 17

Table II Summary of shear strength results obtained by torsion with both glass-ceramics as joining materials

References

-

- ⁹ F. Smeacetto, M. Salvo, M. Santarelli, P. Leone, G.A. Ortigoza-Villalba, A. Lanzini, L.C. Ajitdoss, M. Ferraris, Performance of a glass-ceramic sealant in a SOFC short stack, Int. J. Hydrogen Energy 38 (2013) 588-596.
- ¹⁰ M. Peksen, 3D transient multiphysics modelling of a complete high temperature fuel cell system using coupled CFD and FEM, Int. J. Hydrogen Energy 39 (2014) 5137-5147.
- ¹¹ A. Al-Masria, M. Peksen, K. Khanafer, 3D multiphysics modeling aided APU development for vehicle applications: A thermo-structural investigation, Int. J. Hydrogen Energy 44 (2019) 12094-12107.
- ¹² L. Blum, S.M. Groß, J. Malzbender, U. Pabst, I.C. Vinke, Investigation of solid oxide fuel cell sealing behavior under stack relevant conditions at Forschungszentrum Jülich, J. Power Sources 196 (2011) 7175-7181.
- ¹³ S. Rodríguez-López, J. Wei, K. C. Laurenti, I. Mathias, M. J. Pascual, Mechanical properties of solid oxide fuel cell glass-ceramic sealants in the system BaO/SrO-MgO-B₂O₃-SiO₂, J. Euro. Ceram. Soc. 37 (2017) 3579-3594.
- ¹⁴ M. Fakouri Hasanabadi, M. A. Faghihi-Sani, A. H. Kokabi, S. M. Groß-Barsnick, J. Malzbender, Room- and high-temperature flexural strength of a stable solid oxide fuel/electrolysis cell sealing material, Ceram. Int. 45 (2019) 733-739.
- ¹⁵ J. Malzbender, Y. Zhao, T. Beck, Fracture and creep of glass–ceramic solid oxide fuel cell sealant materials, J. Power Sources 246 (2014) 574-580.
- ¹⁶ Luca Goglio, Monica Ferraris, Bonding of ceramics: An analysis of the torsion hourglass specimen, Int. J. Adhesion and Adhesives, 70 (2016) 46-52.
- ¹⁷ M. Fakouri Hasanabadi, M. A. Faghihi-Sani, A. H. Kokabi, J. Malzbender, The analysis of torsional shear strength test of sealants for solid oxide fuel cells, Ceram. Int. 43 (2017) 12546-1255.
- ¹⁸ M. Fakouri Hasanabadi, A. H. Kokabi, M. A. Faghihi-Sani, S. M. Groß-Barsnick, J. Malzbender, Room- and high-temperature torsional shear strength of solid oxide fuel/electrolysis cell sealing material, Ceram. Int. 45, (2019) 2219-2225.
- ¹⁹ Selçuk, A.; Atkinson, A. Measurement of mechanical strength of glass-to-metal joints. Fuel Cells 2015, 15, 595–603.
- ²⁰ Stephens, E.V.; Vetrano, J.S.; Koeppel, B.J.; Chou, Y.; Sun, X.; Khaleel, M.A. Experimental characterization of glass–ceramic seal properties and their constitutive implementation in solid oxide fuel cell stack models. J. Power Sources 2009, 193, 625–631.
- ²¹ B. Cela Greven, S. Gross-Barsnick, T. Koppitz, R. Conradt, F. Smeacetto, A. Ventrella, M. Ferraris, Torsional shear strength of novel glass-ceramic composite sealants for solid oxide fuel cell stacks, Int. J. Appl. Ceram. Technol. 15 (2018) 286-295.

¹ A. Choudhury, H. Chandra, A. Arora, Application of solid oxide fuel cell technology for power generation—A review, Renewable and Sustainable Energy Reviews 20 (2013) 430-442.

² M.A. Laguna-Bercero, Recent advances in high temperature electrolysis using solid oxide fuel cells: A review, J. Power Sources 203 (2012) 4-16.

³ A. Pandiyan, A. Uthayakumar, R. Subrayan, S.W. Cha, S.B. Krishna Moorthy, Review of solid oxide electrolysis cells: a clean energy strategy for hydrogen generation, Nanomaterials and Energy. 8 (2019) 2–22. doi:10.1680/jnaen.18.00009.

⁴ L. Blum, W.A. Meulenberg, H. Nabielek, R. Steinberger-Wilckens, Worldwide SOFC technology overview and benchmark, I. J. Appl. Cer. Technol. 2 (2005), 482-492

⁵ L. Blum, Q. Fang, L.G.J. de Haart, J. Malzbender, N. Margaritis, N.H. Menzler, SOC development at Forschungszentrum Jülich, ECS Transactions 78 (2017) 1791-1804.

⁶ L. Blum, L.G.J. De Haart, J. Malzbender, N. Margaritis, N.H. Menzler, Anode-supported solid oxide fuel cell achieves 70 000 hours of continuous operation, Energy Technol. 4 (2016) 939-942.

⁷ B. Kuhn, E. Wessel, J. Malzbender, R.W. Steinbrech, L. Singheiser, Effect of isothermal aging on the mechanical performance of brazed ceramic/metal joints for planar SOFC-stacks, Int. J. Hydrogen Energy 35 (2010) 9158-9165.

⁸ Y. Zhao, J. Malzbender, S.M. Groß, The effect of room temperature and high temperature exposure on the elastic modulus, hardness and fracture toughness of glass ceramic sealants for solid oxide fuel cells, J. Euro. Ceram. Soc. 31 (2011) 541-548.

²² F. Smeacetto, A. De Miranda, A. Ventrella, M. Salvo, M. Ferraris, Shear strength tests of glass ceramic sealant for solid oxide fuel cells applications, Adv. Appl. Ceram. 114 (2015) S70-S75.

²³ F. Smeacetto, A. De Miranda, A. Ventrella, M. Salvo, M. Ferraris, Shear strength of glass ceramic sealant for SOFC, J. Am. Ceram. Soc., 97 (2014) 3835–3842.

²⁴ Kerstan et al. Barium silicates as high thermal expansion seals for solid oxide fuel cells studied by high-temperature X-ray diffraction (HT-XRD). https://doi.org/10.1016/j.jpowsour.2011.04.035

²⁵ M.J. Pascual, A. Guillet, A. Durán, Optimization of glass-ceramic sealant compositions in the system MgO-BaO-SiO2for solid oxide fuel cells (SOFC), Journal of Power Sources. 169 (2007) 40–46. doi:10.1016/j.jpowsour.2007.01.040.

²⁶ L. Peng, Q. Zhu, Thermal cycle stability of BaO-B2O3-SiO2 sealing glass, Journal of Power Sources. 194 (2009) 880–885. doi:10.1016/j.jpowsour.2009.06.018.

²⁷ H. Javed, A.G. Sabato, K. Herbrig, D. Ferrero, C. Walter, M. Salvo, Federico Smeacetto Design and characterization of novel glass-ceramic sealants for solid oxide electrolysis cell (SOEC) applications, Int. J. Appl. Ceram. Technol. 15 (2018) 999–1010

²⁸ M. Ferraris, M. Salvo, S. Rizzo, V. Casalegno, S. Han, A. Ventrella, T. Hinoki, Y. Katoh, Torsional shear strength of silicon carbide components pressurelessly joined by a glass-ceramic, Int. J. Appl. Ceram. Technol. 9 (2012) 786-794.

²⁹ M. Ferraris, M. Salvo, V. Casalegno, S. Han, Y. Katoh, H.C. Jung, T. Hinoki, A. Kohyama, Joining of SiC-based materials for nuclear energy applications, J. Nuclear Mater. 417 (2011) 379-382.

³⁰ T. Osipova, J. Wei, G. Pećanac, J. Malzbender, Room and elevated temperature shear strength of sealants for solid oxide fuel cells, Ceram. Int. 42 (2016) 12932-12936.

³¹ J. Wei, G. Pećanac, J. Malzbender, Review of mechanical characterization methods for ceramics used in energy technologies, Ceram. Int. 40 (2014) 15371-15380.

³² M. Ferraris, A. Ventrella, M. Salvo, D. Gross, Shear strength measurement of AV119 epoxy-joined SiC by different torsion tests, Int. J. Appl. Ceram. Technol. 11 (2014) 394-401.

³³ S. De La Pierre, T. Scalici, P. Tatarko, A. Valenza, L. Goglio, D. Paolino, M. Ferraris, Torsional shear strength and elastic properties of adhesive bonded glass-to-steel components, paper under revision.

³⁴ Javed, H.; Sabato, A.G.; Dlouhy, I.; Halasova, M.; Bernardo, E.; Salvo, M.; Herbrig, K.; Walter, C.; Smeacetto, F. Shear Performance at Room and High Temperatures of Glass–Ceramic Sealants for Solid Oxide Electrolysis Cell Technology. *Materials* 2019, *12*, 298. doi:10.3390/ma12020298